Rare Metal Materials and Engineering
Volume 54, Issue 3, March 2025
Available online at www.rmme.ac.cn

Science Press

Cite this article as: Hu Jianian, Zhou Zizheng, Li Yidi, et al. Design and Dynamic Experiment of Al-Cu Graded Materials Impactor with Strain Rate of 10^4 – 10^5/s[J]. Rare Metal Materials and Engineering, 2025, 54(03): 581-586. DOI: https://doi.org/10.12442/j.issn.1002-185X.20240293.

ARTICLE

Design and Dynamic Experiment of Al-Cu Graded Materials Impactor with Strain Rate of 10^4 – 10^5/s

Hu Jianian[1,2], Zhou Zizheng[1,2], Li Yidi[1,2], Chen Xiang[1,2], Yang Gang[1,2], Liu Jintao[3], Zhang Jian[4]

[1] State Key Laboratory of Precision Blasting, Jianghan University, Wuhan 430056, China; [2] Hubei Key Laboratory of Blasting Engineering, Jianghan University, Wuhan 430056, China; [3] Luoyang Ship Material Research Institute, Luoyang 471023, China; [4] State Key Laboratory of Advanced Technology for Materials Synthesis and Processing, Wuhan University of Technology, Wuhan 430070, China

Abstract: Based on simplified calculations of one-dimensional wave systems, loading pressure platform curves of Al-Cu gradient materials (GMs) impactor were designed. The Al-Cu GMs were prepared using tape-pressing sintering, and their acoustic properties were characterized to match the design path. The parallelism of the Al-Cu GM was confirmed using a three-dimensional surface profilometry machine. A one-stage light-gas gun was used to launch the Al-Cu GM, impacting an Al-LiF target at a velocity of 400 m/s. The results of the experimental strain rate demonstrate that the Al-Cu GMs can realize the precise control of the strain rate within the range of 10^4–10^5/s in the high-speed impact experiments.

Key words: high strain rate; Al-Cu graded materials; impactor; acoustic impedance; gas gun experiment

1 Introduction

The mechanical properties of materials under various strain rates are pivotal for their application in diverse working environments[1–3]. Traditional static mechanical property tests typically capture the mechanical response behavior only within lower strain rate ranges of 10^{-5} – 10^1/s. However, understanding material dynamics and solid-state deformation mechanisms under high strain rates is still a significant research area for decades[4–9]. The response of materials to impacts and other high strain promotes the development of numerous theories, ranging from empirical models to the latest physical models[10–13]. The duration of loading at ultra-high strain rate is notably brief and the strain stress stability is more important compared to that at low strain rate. Therefore, to achieve precise control of stress, it is necessary to test samples at relatively constant strain rates.

Split Hopkinson pressure bar (SHPB) experiments and gas gun experiments are two common methods used for conducting experiments at relatively high strain rates. In SHPB experiments, the testing strain rate typically falls within the range of 10^1 – 10^3/s[14–16]. And the strain rate of gas gun experiments is in the range of 10^6 – 10^9/s. However, there is little attention paid to strain rates between 10^4/s and 10^5/s, which are widely used in research on explosive welding and blasting proximity[17–19]. Although the stress-strain curves produced by SHPB experiments closely resemble the ideal elastoplastic behavior with approximately constant strain rates, some researchers argue that the effect of strain rate on metal materials is primarily sensitive to the logarithm of variability. Consequently, they assume that modest changes in strain rate during experiments may not significantly influence the test results[20]. However, as the demand for more constitutive equations of reliable material increases, there is a growing awareness of the importance of such small differences[21–22]. Materials such as high polymers and nano-materials exhibit high sensitivity to strain rate, and even slight variations in strain rate can induce significant differences in stress-strain curves and microstructure[23–24]. Thus, there is an urgent need to conduct experiments with high strain rates of

Received date: May 17, 2024
Foundation item: Natural Science Foundation of Hubei Province (2024AFB432); National Natural Science Foundation of China (52171045, 12302436, 52302095); Research Fund of Jianghan University (2023JCYJ05)
Corresponding author: Liu Jintao, Ph. D., Luoyang Ship Material Research Institute, Luoyang 471023, P. R. China, E-mail: liujintao725@163.com

10^4–10^5/s to meet the demands of sophisticated tests.

Graded material (GM) impactors were demonstrated to effectively reduce the strain rates in dynamic experiments[25–26]. Previous studies focused on preparing several types of GMs, including Mg-Cu, W-Cu, and W-Cu-Mg, to facilitate dynamic impacting[26–28]. However, designing loading paths to achieve the desired loading strain rate was proven to be a challenge, particularly because element Mg with hexagonal close-packed structure is susceptible to phase transitions. To obtain reliable dynamic experimental results, Al-Cu GMs were selected for dynamic experiments due to the favorable properties and low susceptibility to phase transitions.

2 Experiment

By meticulously controlling the composition and thickness of the GMs using one-dimensional wave calculations, the corresponding loading path was derived, which was characterized by a ramp loading before the initial shock loading. Several loading path curves were designed for impacting an Al target and then transformed into various Al-Cu GM structures using one-dimensional wave calculations. Subsequently, the corresponding Al-Cu GMs were prepared through tape casting and hot press sintering techniques. The physical properties of Al-Cu GMs were predicted based on the monolithic properties, such as density and acoustic impedance. The effectiveness of the graded structures was assessed using a three-dimensional surface profilometry machine. And then the prepared GMs were employed to impact an Al-LiF target at a velocity of 400 m/s using a one-stage light-gas gun. Experimental pressure curves were meticulously measured using a photon Doppler velocimeter and compared to the designed pressure curve.

Al-Cu GMs with diverse loading paths were designed and the impedance-thickness distribution corresponding to each path was derived using the MLEP (2015SR065998) software developed by China Academy of Engineering Physics. And then the variations in loading pressure and strain rate associated with these different loading paths were calculated. Al-Cu GMs with the designed impedance-thickness distribution were prepared by adjusting the density and acoustic velocity of the single-layer materials in accordance with Eq.(1)[25]:

$$Z=\rho v \quad (1)$$

where Z represents the impedance-thickness distribution; ρ and v are the density and acoustic velocity, respectively. Single-layer thickness was controlled through mass. Firstly, metal powder and dispersant were placed in a zirconia ball milling tank, and then ethanol and butanone solvents were added. The mixture was stirred in a three-dimensional ball mill at 240 r/min for 12 h. Subsequently, corresponding binders and plasticizers were added and mixed for 12 h at the same speed, resulting in Al-Cu casting slurries with various composition. These slurries were used to form Al-Cu casting films using double scrapers. The thickness of the films after drying was controlled by adjusting the height of scrapers. Then, the dried Al-Cu casting films were cut into wafers with predetermined diameter, stacked sequentially, and pressed into cast blanks by a tablet press under the stress of 100 MPa. Finally, the thickness was meticulously controlled through rigorous mass assurance processes. The scanning electron microscope (SEM, Thermo Fisher, Quanta250) was used to characterize the graded structure of Al-Cu GMs. The flatness of the Al-Cu GM was assessed using the three-dimensional optical profiler (ST400, American Nanovea Company), which included measurements of parallelism and detection of internal defects. Subsequently, the Al-Cu GMs served as impactors and were launched at high velocity for dynamic experiments using a gas gun, as depicted in Fig.1. Sample data were collected from the target comprising a Al baseplate with the thickness of 2.0 mm and a LiF window. Changes in pressure and strain rate were recorded at the interface of the Al-LiF window, providing valuable insights into the dynamic behavior of the system.

3 Results and Discussion

To demonstrate the effectiveness of the experimental design, we devised several paths aiming to attain the maximum pressure of 5 GPa. The relationship between pressure and time is as follows[26]:

$$p(t)=p_0+A(t)^P \quad (2)$$

where $p(t)$ is a function of pressure changed with time, p_0 is the initial pressure, P is the pressure loading index, and A is the proportionality coefficient, which has different values in different pressure paths. Obviously, any loading path can be obtained through the change of P value. The initial pressure p_0 of Al-Cu GMs can be determined from the highest pressure of 3.56 GPa. Fig. 2 illustrates several distinct loading paths designed by the principles.

Using one-dimensional wave calculation, the pressure curve can be transformed into an impedance-thickness curve specific to the Al-Cu GMs. Subsequently, the impedance-thickness curve can be further converted into a composition-thickness curve of the Al-Cu GMs according to the mixing rule of impedance calculation, as depicted in Fig. 3. Once the composition-thickness curve is established, GMs can be produced in accordance with these curves. The design of the components determines the impedance-thickness distribution, which can be calculated from the corresponding pressure curve by MLEP software.

Fig. 4 depicts the pressure and strain rate curves derived from one-dimensional wave calculations[26]. Analysis of the

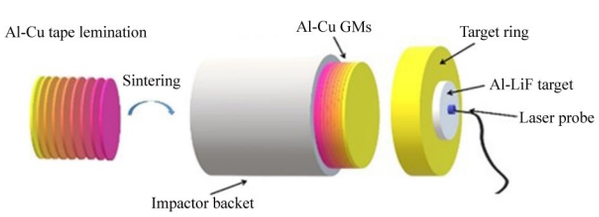

Fig.1 Schematic diagram of dynamic experimental process

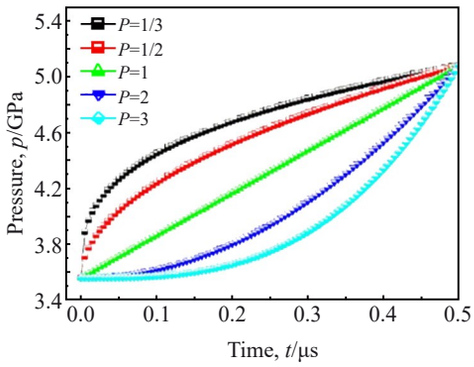

Fig.2 Pressure curves of Al-Cu GMs with different *P* values

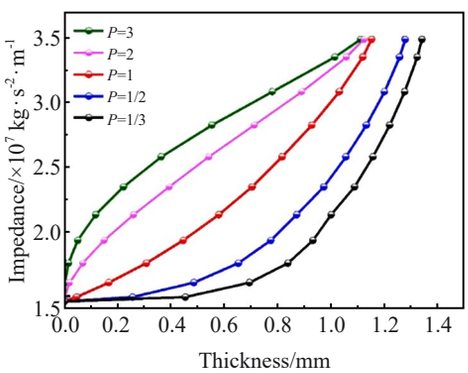

Fig.3 Impedance-thickness curves of Al-Cu GMs with different *P* values

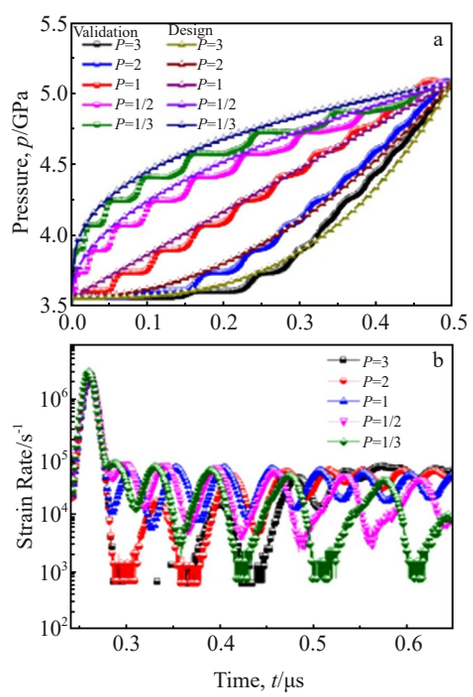

Fig. 4 Validation and design pressure curves with different *P* values (a); strain rate-time curves calculated from GM structure distribution (b)

results reveals that the initial higher strain rate corresponds to the initial impact pressure of the front Al shock loading. Subsequently, the strain rate of the target falls within the range of 10^3–10^5/s, owing to the pressure platform generated by the Al-Cu stacked structure design. The pressure platform means that the GMs are loaded with each layer appearing a corresponding constant value to the corresponding pressure. When the pressure loading index is 1, the strain rate is confined within a relatively narrow range of 10^4 – 10^5/s. Consequently, the corresponding Al-Cu GMs were prepared and experiments were conducted using the gas gun.

The microstructures of various Al-Cu GMs are depicted in Fig. 5. Cu particles are shown in white and Al particles are shown in gray. Both Al and Cu particles are uniformly distributed with different pressure loading indexes without discernible pores, which indicates that Al and Cu particles have high densification and effective dispersion. The interfaces of the Al-Cu GMs are distinctly defined, facilitating the calculation of impedance-thickness distribution for the GMs based on their respective locations.

To assess the impact effect on the target, different curves of the GMs obtained in the experiment are presented in Fig. 6. The error between the experimental impedance values and the designed values for the Al-Cu GMs is within 4%. The thickness of the film was meticulously controlled using the density obtained from the homogeneous monolayer materials to adjust the mass and to ensure a constant reduction of mass during the removal of polymer additives. As shown in Fig. 5a, the thickness of the *n*th layer for different Al-Cu GMs is represented by d_n. The average thickness of the films is 50±2.5 μm with the error less than 5%. The thickness of the GMs can be further adjusted based on precise control of mass.

The impact design results and structural characterization findings demonstrate that the strain rate along the loading path can be effectively controlled within the designated range when *P*=1. Surface parallelism of the corresponding Al-Cu GMs characterized by a three-dimensional profiler is depicted in Fig. 7. Apparent differences in flatness of the GMs indicate variations in internal coefficients of thermal expansion and stress levels. From the two-dimensional height difference map of the Al surface in Fig. 7a, different colors represent various height differences. The Al surface appears lower in the center and higher around the edges, which indicates the Al surface is concave while the Cu surface appears convex. The curvature of both surfaces is approximately 20 μm. Ensuring good surface parallelism is crucial for maintaining the accuracy of data in impact experiments.

Fig. 8a illustrates the pressure curve for the Al-Cu GMs, impacting an Al target of 2 mm equipped with a LiF window when the pressure loading index is 1. The pressure within the Al target was derived from initial data obtained via laser probe measurements. Initially, the particle velocity exhibits an abrupt shock impact within 0.1 μs, followed by a pressure plateau of 3.56 GPa, corresponding to the structure of the pure Al layer Subsequently, a smooth wave platform ramps up from 3.56 GPa to 5.0 GPa, representing each layer of GMs

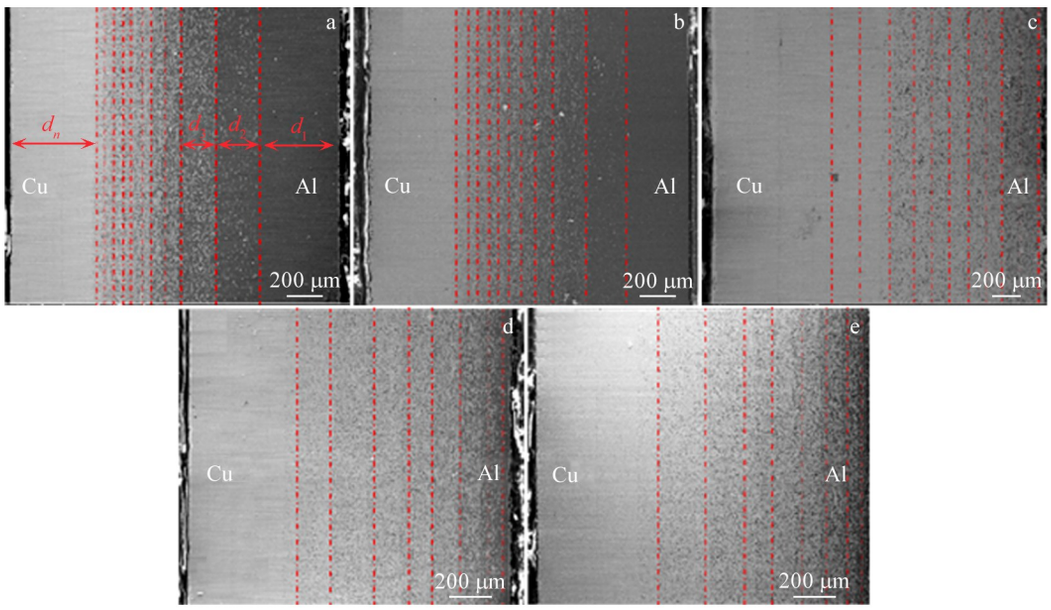

Fig.5 Microstructures of Al-Cu GMs with different *P* values: (a) *P*=3; (b) *P*=2; (c) *P*=1; (d) *P*=1/2; (e) *P*=1/3

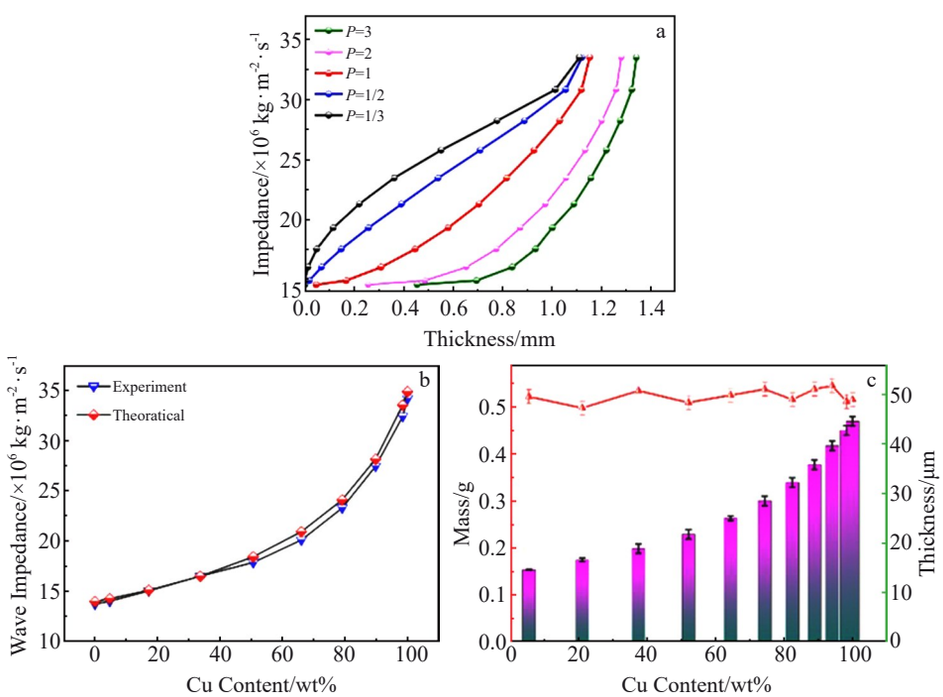

Fig.6 Impedance-thickness curves of Al-Cu GMs with different *P* values (a); comparison between experimental and theoretical values of wave impedance curves (b); layer thickness of films for Al-Cu GMs obtained by mass measurement (c)

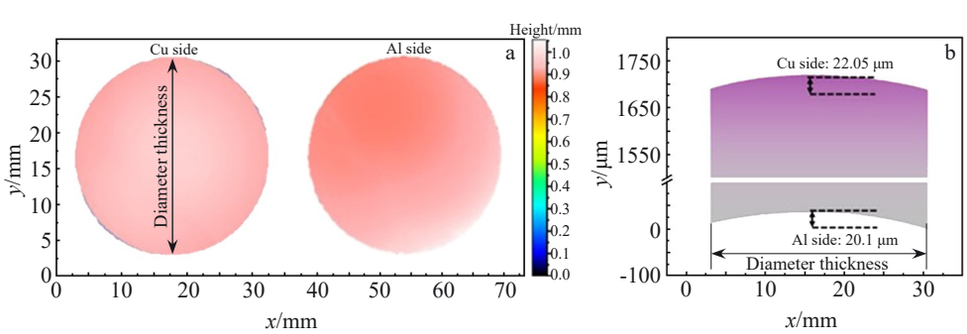

Fig.7 Two-dimensional height difference maps of Cu and Al surface (a); flatness schematic diagram of Al-Cu GMs (b)

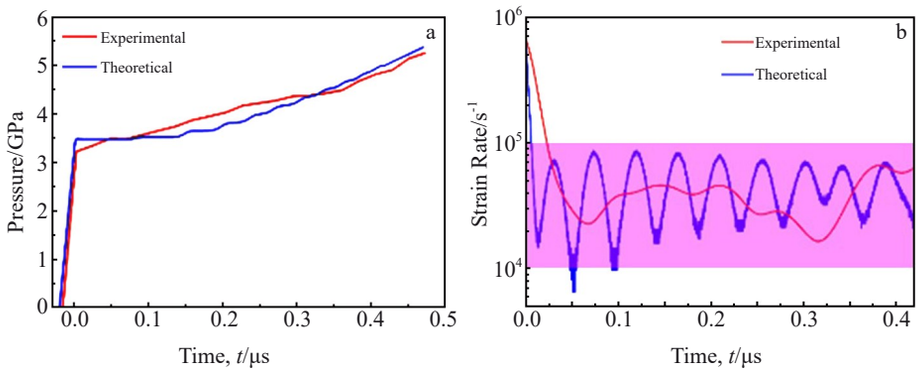

Fig.8 Comparison between experimental and theoretical curves of pressure (a) and strain rate (b)

up to the Cu layer. The pressure data obtained from the gas gun experiment align well with the initially designed pressure curve. The differences between the designed and experimental pressure data can be attributed to the impedance-thickness data, which exhibit a relatively low uncertainty below 5%, primarily due to impedance changes caused by diffusion at the sintered interface within the Al-Cu GMs. Fig. 8b displays the strain rate of the target. The experimental strain rate is confined within a narrow range of $10^4 – 10^5$/s. Notably, the experimental strain rate appears smoother than the designed theoretical curve due to interfacial diffusion within the Al-Cu GMs.

In conclusion, this research demonstrates the feasibility and effectiveness of using Al-Cu GMs to achieve precise control of strain rates in high-speed impact experiments, thereby contributing to advancements in materials testing and characterization under dynamic loading conditions.

4 Conclusions

1) The methodology to achieve a strain rate range of $10^4 – 10^5$/s for impacting an Al target using Al-Cu GMs is successfully designed and implemented. Through the conversion from pressure distribution curves into impedance-thickness distribution curves of Al-Cu GMs based on the principle of GM wave system propagation, a suitable curve corresponding to the desired strain rate range is selected.

2) The Al-Cu GMs are meticulously prepared by tape casting method, which ensures the control of wave impedance and thickness with an error under 5%. Although the prepared Al-Cu GMs exhibit low flatness and obvious internal graded structure, they effectively transform the designed pressure curves into experimental results. The pressure curves obtained from experimental samples closely resemble the designed curves, displaying a smooth wave platform rising from 3.56 GPa to 5.00 GPa, while the strain rate remains within the narrow range of 10^4–10^5/s.

References

1 Liu H, Pang Y Z, Su D D *et al*. *Applied Sciences*[J], 2023, 13(16): 9214
2 Wang M Z, Li J L, Zhang J Z *et al*. *Journal of Materials Engineering and Performance*[J], 2020, 29(35): 506
3 Gholizadeh R, Shibata A, Tsuji N. *Materials Science and Engineering A*[J], 2020, 790: 139708
4 Estrada J B, Barajas C, Henann D L *et al*. *Journal of the Mechanics and Physics of Solids*[J], 2018, 112: 291
5 Akhondzadeh S, Kang M, Sills R B *et al*. *Acta Materialia*[J], 2023, 250: 118851
6 Wang W, Politis N J, Wang Y P *et al*. *International Journal of Machine Tools and Manufacture*[J], 2022, 180: 103930
7 Yuan L, Xiong J T, Peng Y *et al*. *Vacuum*[J], 2020, 173: 109120
8 Liu J, Liu H B, Kaboglu C *et al*. *Applied Composite Materials*[J], 2019, 26: 1389
9 Wang Mingzhi, Wang Chuanting, He Yong *et al*. *Rare Metal Materials and Engineering*[J], 2021, 50(2): 627 (in Chinese)
10 Ge J P, Saiidi M S. *Shock and Vibration*[J], 2018(3): 4276167
11 Suhir E, Ghaffarian R. *Journal of Applied Mathematics and Mechanics*[J], 2017, 97(6): 699
12 Long Kui, Deng Yongjun, Chen Xiaowei *et al*. *Rare Metal Materials and Engineering*[J], 2022, 51(10): 3826 (in Chinese)
13 Heshmati M, Zamani A J, Mozafari A. *Materialwissenschaft und Werkstofftechnik*[J], 2017, 48(2): 106
14 Fu Y S, Chen S B, Zhao P L *et al*. *Materials*[J], 2023, 16(24): 7659
15 Khan M M, Kumar A, Iqbal M A. *Mechanics of Solids*[J], 2024, 58(9): 3315
16 Price M C, Cole M J, Harriss K H *et al*. *International Journal of Impact Engineering*[J], 2024, 184: 104828
17 Luo N, Liang H L, Sun X *et al*. *Composite Interfaces*[J], 2021, 28(6): 609
18 Yang M, Ma H H, Shen Z W *et al*. *Materials & Design*[J], 2020, 186: 108348
19 Hu J N, Jia Y S, Chen X *et al*. *Journal of Materials Research and Technology*[J], 2023, 25: 4720
20 Shen Z X, Zou G T, Dong Y *et al*. *Journal of Materials Research and Technology*[J], 2024, 28: 2815
21 Yamada H, Sakai T, Ogasawara N *et al*. *Ocean Engineering*[J], 2023, 287: 115719
22 Pandey A, Bhandari L, Gaur V. *Engineering Applications of*

Artificial Intelligence[J], 2024, 128: 107534

23 Kim J, Lee C Y, Rho H *et al*. *Journal of Nuclear Materials*[J], 2024, 592: 154947

24 Schaffar G J K, Tscharnuter D, Maier-Kiener V. *Materials & Design*[J], 2023, 223: 112198.

25 Martin L P, Orlikowski D, Nguyen J H. *Materials Science and Engineering A*[J], 2006, 427(1–2): 83

26 Martin, L P, Patterson J R, Orlikowski D *et al*. *Journal of Applied Physics*[J], 2007, 102(2): 023507

27 Krone R T, Martin L P, Patterson J R *et al*. *Materials Science and Engineering A*[J], 2008, 479(1–2): 300

28 Vogler T J, Ao T, Asay J R. *International Journal of Plasticity*[J], 2009, 25(4): 671

加载应变率为10^4–10^5/s的Al-Cu梯度飞片材料的设计与动态实验

胡家念[1,2]，周子正[1,2]，李一迪[1,2]，陈　翔[1,2]，杨　刚[1,2]，刘金涛[3]，张　建[4]

(1. 江汉大学 精细爆破国家重点实验室，湖北 武汉 430056)

(2. 江汉大学 爆破工程湖北省重点实验室，湖北 武汉 430056)

(3. 中国船舶集团有限公司第七二五研究所，河南 洛阳 471023)

(4. 武汉理工大学 材料复合新技术国家重点实验室，湖北 武汉 430070)

摘　要：基于梯度材料一维波系作用的简化算法设计了Al-Cu梯度飞片材料的加载压力曲线。通过热压法制备相应的Al-Cu梯度材料，其表征后的阻抗性能与设计路径相匹配。采用三维表面轮廓仪检测Al-Cu梯度材料的平行度，并利用一级气炮以400 m/s的速度发射Al-Cu梯度材料冲击Al-LiF靶材。该实验应变率的结果证明了Al-Cu梯度材料能够实现高速冲击实验中应变速率在10^4–10^5/s范围的精确控制。

关键词：高应变率；Al-Cu梯度材料；飞片；波阻抗；气炮实验

作者简介：胡家念，男，1993年生，博士，江汉大学精细爆破国家重点实验室，湖北 武汉 430056，E-mail：hjn@jhun.edu.cn